INFECTION AND IMMUNITY, Jan. 1985, p. 52–60
0019-9567/85/010052-09$02.00/0
Copyright © 1985, American Society for Microbiology
Vol. 47, No. 1

Mechanism of Membrane Damage by Streptolysin-O

SUCHARIT BHAKDI,[1]* JØRGEN TRANUM-JENSEN,[2] AND ANDREAS SZIEGOLEIT[1]

Institute of Medical Microbiology, University of Giessen, D-6300 Giessen, Federal Republic of Germany,[1] and Anatomy Institute C, University of Copenhagen, DK-2200 Copenhagen N, Denmark[2]

Received 26 July 1984/Accepted 13 September 1984

Streptolysin-O (SLO) is a thiol-activated, membrane-damaging protein toxin of M_r 69,000 that is produced by most strains of β-hemolytic group A streptococci. Native, primarily water-soluble toxin molecules bind to cholesterol-containing target membranes to assemble into supramolecular curved rod structures (25 to 100 nm long by ca. 7.5 nm wide), forming rings and arcs that penetrate into the apolar domain of the bilayer. Electron microscopic analyses of toxin polymers in their native and reconstituted membrane-bound form indicate that the convex surface of the rod structures is a hydrophobic, lipid-binding domain, whereas the concave surfaces appear to be hydrophilic. The embedment of the rings and arcs generates large transmembrane slits or pores of up to 30-nm diameter that can be directly visualized by negative staining and freeze-fracture electron microscopy. SLO oligomers were isolated in extensively delipidated form in detergent solution, and cholesterol was found not to detectably contribute to the observed rod structures. The rods are stable structures that resist prolonged exposure to trypsin and chymotrypsin. They can be reincorporated into cholesterol-free phosphatidylcholine liposomes to generate lesions identical to those observed on erythrocytes lysed by native SLO. Thus, although cholesterol plays a key role in the initial binding of SLO to the membrane, it does not directly participate in the formation of the membrane-penetrating toxin channels. Membrane damage by SLO is basically analogous to that mediated by previously studied channel formers, namely, the C5b-9 complement complex and staphylococcal α-toxin.

Lancefield group A β-hemolytic streptococci are the major human pathogens of the genus *Streptococcus*, and streptolysin-O (SLO) is considered to be one of the important toxins that is produced by most strains. SLO is the prototype of the oxygen-labile, thiol-activated bacterial toxins which represent a category encompassing at least 15 exotoxins produced by various gram-positive bacteria including tetanolysin, cereolysin, listeriolysin, and perfringolysin (1, 2, 4, 5, 25). All of these primarily water-soluble toxins share the following properties. They consist of single polypeptide chains in the M_r range 50,000 to 80,000; they are reversibly inactivated by atmospheric oxygen and require the presence of a reducing agent for maximal expression of biological activity; they invoke membrane damage after binding to surface-exposed membrane cholesterol; and membrane damage has in several cases been shown to be accompanied by the appearance of circular, semicircular, and compound arc structures visible by electron microscopy (4, 12, 13, 15, 22, 25, 26). These structures are widely believed to represent toxin-cholesterol complexes (1, 4, 15). In the case of SLO, damaged membranes have been shown to exhibit large, functional holes that allow for the passage of very large molecules with molecular diameters exceeding 15.0 nm (11, 14). It has earlier been proposed that extraction or sequestration of membrane cholesterol through its complexation with SLO molecules is responsible for the generation of these functional lesions, but the precise nature of the SLO-induced arcs and rings and the nature of the membrane lesions have eluded definition (1, 4, 5, 15, 26).

In the course of our studies on channel-forming proteins, we have isolated and characterized the membrane-damaging C5b-9 complement complex and the channel-forming hexamer of staphylococcal α-toxin (9, 17, 28). Common to these proteins that are hydrophilic in their native state is their ability to self-associate on and in a target bilayer to form supramolecular, amphiphilic ring structures whose embedment within the membrane generates transmembrane channels (9, 9a, 17). In this paper, we report on the isolation and characterization of SLO oligomers from target membranes. We provide evidence that, as inferred by Duncan and colleagues from their earlier studies (11, 14, 15), these toxin oligomers most probably form very large transmembrane pores in the target bilayer. Thus, membrane damage by this toxin follows the same basic principle of channel formation as found for complement and α-toxin.

(A preliminary report on this subject has been presented previously [10].)

MATERIALS AND METHODS

SLO was purified from culture supernatants of group A streptococci (Richards strain) by a procedure developed in our laboratory (8). Experiments were performed with purified native toxin (SLO_a, M_r 69,000); degraded, hemolytically active toxin (SLO_b, M_r 57,000); or preparations containing mainly SLO_a and SLO_b forming a minor component (less than 10%). The same results were obtained with all preparations. Assays for protein and hemolytic activity were performed as described previously (8).

Isolation of membrane-bound SLO. One volume of rabbit or human erythrocytes (10^9 cells per ml) was incubated with 1 volume of SLO (50 to 80 μg/ml) plus 5 mM dithiothreitol for 1 to 2 min at 37°C. Lysis was complete within seconds. The membranes were pelleted at 25,000 × *g* for 15 min at 4°C (Sorvall RC2B centrifuge, rotor SS34) and washed three times with 5 mM phosphate buffer, pH 8.0. Binding of SLO to membranes was virtually quantitative as determined by hemolytic titrations and sodium dodecyl sulfate-polyacrylamide gel electrophoresis (SDS-PAGE) of lysis supernatants. Washed membranes (ca. 5 to 6 mg of protein per ml) were quantitatively solubilized by the addition of solid sodium deoxycholate (DOC; E. Merck AG, Darmstadt,

* Corresponding author.

Federal Republic of Germany) to a final concentration of 250 mM. Samples (1 ml) were applied to linear 10 to 43% (wt/wt) sucrose density gradients containing 6.25 mM DOC as described previously for the isolation of C5b-9(m) from membranes (7). After centrifugation at 150,000 × *g* for 16 h at 4°C (Beckmann ultracentrifuge; rotor type SW41 Ti; 12-ml gradient volumes), 10 or 20 equal fractions were collected from the bottom of the tubes. Control membranes lysed with 5 mM phosphate buffer (pH 8.0) were processed in parallel as controls. The SLO oligomers were recovered in high-molecular-weight fractions well separated from the bulk of erythrocyte membrane proteins (see below). Antisera were raised in rabbits by following published immunization schemes (19), injecting animals with purified SLO that had been isolated from lysed rabbit erythrocytes.

EDTA extraction experiments. Washed and pelleted membranes were extracted with dilute EDTA by suspension in 5 volumes of 1 mM EDTA (pH 8.0) at 37°C for 3 h, and then pelleted at 150,000 × *g* for 60 min at 4°C (Beckmann ultracentrifuge, SW41 Ti rotor). EDTA-extracted membrane pellets were solubilized with DOC. Both the solubilized membranes and the aqueous EDTA extracts were applied to sucrose density gradients and centrifuged as described above. These experiments were performed to determine the elutability of SLO oligomers from membranes with dilute EDTA.

Membrane reconstitution experiments. Fractions containing SLO from sucrose density gradients were admixed with solutions of egg lecithin (10 mg/ml; type V-E; Sigma Chemical Co., Munich, Federal Republic of Germany) in 50 mM DOC at protein/lipid ratios (wt/wt) of 1:20 to 1:30. After removal of DOC by dialysis against 20 mM Tris–100 mM NaCl–7.5 mM NaN_3 buffer (pH 8.0) (36 h, 4°C), lipid vesicles were isolated by flotation through sucrose (9).

Analytical procedures. SDS-PAGE was performed on 1.5-mm gel slabs as described previously, using 10% separation and 5% stacking gels containing 6 M urea (7, 17). Lipids and cholesterol were detected by applying 10-μl samples directly to thin-layer silica plates and chromatographing them in chloroform-methanol-water (65:35:5, vol/vol/vol). The plates were developed by spraying them with 5% H_2SO_4 in ethanol and heating them on a hot plate. Cholesterol was additionally determined enzymatically with a commercially available kit from Boehringer Mannheim (Mannheim, Federal Republic of Germany). For these analyses, SLO-containing fractions recovered from the sucrose density gradients were pooled, dialyzed overnight to remove sucrose and detergent, and lyophilized. The lyophilized material was taken up in 100 μl of saline, and cholesterol determinations were performed on the total sample following the manufacturer's instructions.

Electron microscopy. Samples of detergent-solubilized, membrane-derived SLO from sucrose density gradients were dialyzed against buffer containing 10 mM DOC to remove sucrose before negative staining with 2% sodium silicotungstate or 1% uranyl sulfate on thin carbon-coated Formvar films as detailed previously (28). Samples of membrane-reconstituted SLO were processed similarly.

Sheep, rabbit, or human erythrocytes lysed with dithiothreitol-activated SLO (50 μg of toxin per 10^9 cells; 5 mM dithiothreitol) and washed in 5 mM phosphate buffer (pH 8.0) were negatively stained with 2% sodium silicotungstate or phosphotungstate with or without prior fixation in OsO_4 as detailed previously (8a). For freeze-fracture, membranes were fixed for 4 to 8 h at 4°C in 2.5% glutaraldehyde in 50 mM phosphate buffer (pH 7.2), or they were frozen directly in 5 mM phosphate buffer without any additional treatment. Fixed membranes were gently sedimented and resuspended in 30% (vol/vol) glycerol as cryoprotectant for standard freeze-fractures, or they were washed in 5 mM phosphate and frozen without cryoprotectants for deep freeze-etchings. Small drops of packed membranes were applied to gold disks and frozen by immersion in Freon 22 or propane, cooled by liquid nitrogen. Freeze-fractures and etchings were performed in a Balzers BAF 301 unit equipped with Pt-C and C electron guns, at 10^{-7} to 10^{-6} torr and −105°C (−100°C for etchings). Fractures were produced by a knife, rotary shadowed with Pt-C at 25°C relative to the specimen plane, and reinforced by vertical C evaporation. Replicas were rinsed in chromosulfuric acid and collected on naked grids.

Controls for the membrane preparations were hypotonically lysed erythrocyte membranes treated with dithiothreitol and processed in parallel with the SLO-treated membranes.

Specimens were examined and photographed in a JEOL 100 CX electron microscope, operated at 80 kV.

RESULTS

SDS-PAGE of SLO-treated erythrocyte membranes. Figure 1 depicts the SDS-PAGE patterns of control human erythrocyte membranes (lane a) and of SLO-treated membranes (lane b). It is apparent that cell lysis by SLO under the given conditions is not accompanied by any detectable alteration in the polypeptide composition or degradation of membrane proteins. SLO-treated membranes exhibited strengthening of one polypeptide band in the region of 70,000 to 80,000

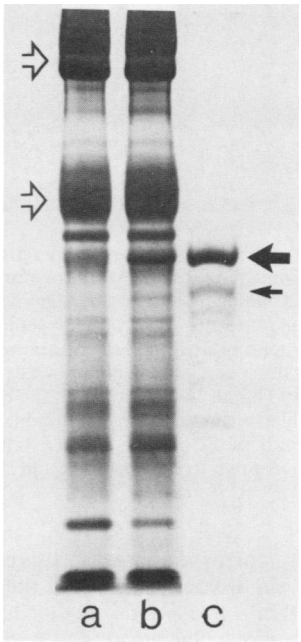

FIG. 1. SDS-PAGE of control human erythrocyte membrane proteins (lane a), SLO-treated membranes (lane b), and purified SLO (lane c; 15 μg of protein applied). The toxin preparation contained over 90% native SLO (SLO_a [see reference 7]; bold arrow; M_r 69,000) and some degraded toxin (SLO_b; small arrow; M_r 57,000). Other protein bands represent contaminants. Toxin-lysed membranes exhibit no alteration of the original polypeptide banding pattern. The protein bands corresponding to bound SLO_a and SLO_b can be seen superimposed on the membrane protein pattern. Open arrows point to the spectrins (top arrow) and the major integral band 3 protein (lower arrow).

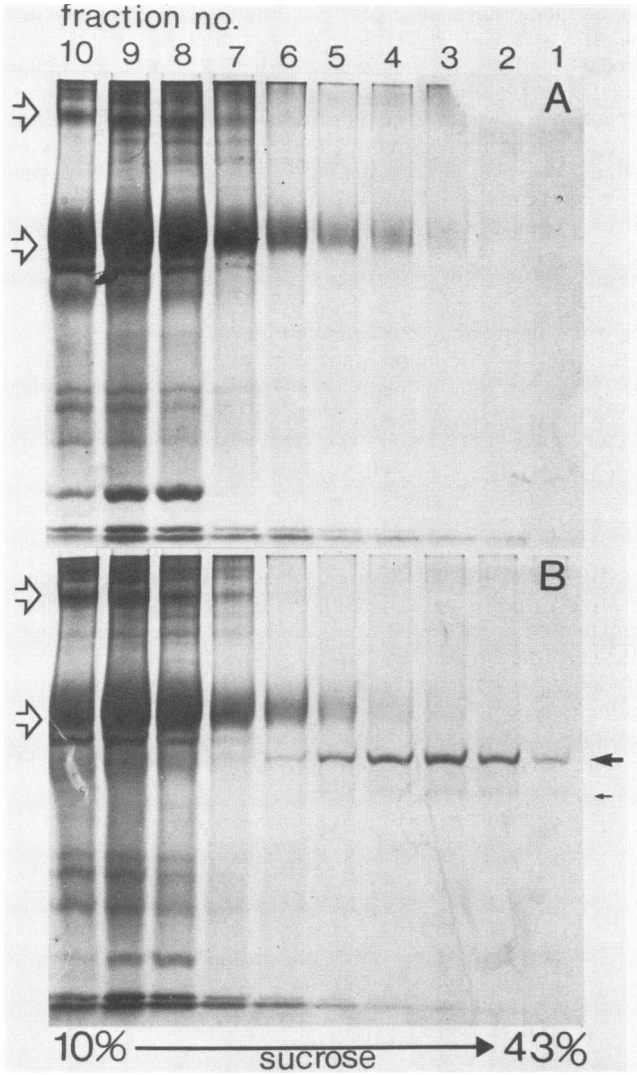

FIG. 2. Isolation of SLO oligomers from rabbit target erythrocyte membranes. Control or toxin-treated membranes were solubilized in 250 mM DOC and centrifuged through linear, DOC-containing sucrose density gradients (direction of sedimentation, left to right). Ten equal fractions were collected, and samples were analyzed by SDS-PAGE. (A) Control membranes; (B) SLO-treated membranes. The SLO bands (solid arrows to the right) are observed in the high-molecular-weight regions (fractions 1 to 5 and 6), separated from the bulk of the contaminating erythrocyte membrane proteins. Open arrows point to the spectrins and band 3 protein (see Fig. 1).

molecular weight, corresponding to native SLO (lane c). There was also a slight strengthening of the 70,000-molecular-weight band that corresponds to the degraded form of SLO (SLO_b). The molecular weights of native SLO (SLO_a) and degraded SLO (SLO_b) have been previously determined by ultracentrifugation to be 69,000 and 57,000, respectively (8).

Isolation of membrane-bound SLO. Initial experiments showed that membrane-bound SLO was very poorly solubilized by Triton X-100. Membrane solubilization with very high DOC concentrations, however, led to the isolation of SLO from the membrane in a simple, one-step procedure. Figure 2A shows SDS-PAGE patterns of sucrose density gradient fractions obtained from control, DOC-solubilized erythrocyte membranes. The bulk of membrane proteins is recovered in the upper half of the gradient. Figure 2B shows a parallel fractionation of SLO-treated membranes. The major and minor SLO protein bands are seen to have sedimented faster than other membrane proteins and are recovered in high-molecular-weight fractions covering a broad range corresponding to 20S to 40S. This would correspond to composite protein-detergent molecular weights ranging from about one million to several million.

Fractions containing the SLO bands were pooled and used for immunization. The antisera obtained reacted with the same two SLO bands in an immunoblot analysis of bacterial culture supernatants and of SLO-treated membranes (8).

Non-extractability of membrane-bound SLO by dilute EDTA. Treatment of erythrocyte membranes with dilute EDTA at pH 8.0 selectively extracts peripheral membrane proteins (16, 27). Figure 3A shows SDS gels of an EDTA extract of SLO-treated human erythrocyte membranes after centrifugation through a DOC-containing sucrose density gradient. The presence of peripheral membrane proteins including the spectrins is apparent, whereas band 3 protein (major integral membrane protein [27]) was not contained in the extract. It can be seen that no protein bands corresponding to SLO were detected in the high-molecular-weight fractions (cf. Fig. 2 and 3B). In contrast, DOC-solubilized EDTA-membrane pellets contained all the SLO and band 3 proteins (Fig. 3B). Membrane pellets harvested after EDTA extraction were three- to fivefold concentrated in SLO over the starting membrane suspension. The concentration of membrane-derived SLO could thus conveniently be increased for examination in the electron microscope and for membrane reconstitution studies.

Additional experiments were performed with nonfractionated, concentrated culture supernatants containing SLO. We found that brief treatment (40 to 60 s) at 37°C of cells with such supernatants (hemolytic titers, 1:2,000 [8]) led to identical results, and SLO could be isolated from such membranes equally well. Prolonged incubations had to be avoided because of the presence of proteases and phospholipases in the culture supernatants that caused severe fragmentation of the target membranes.

Absence of detectable lipid in SLO-preparations. By thin-layer chromatography, we found that lipids were apparently quantitatively recovered both in the control and in SLO-treated membrane samples in the upper four to five fractions of the DOC-sucrose density gradients, and no lipids could be detected in the sucrose density gradient fractions containing the isolated SLO oligomers. Additionally, enzymatic determinations of cholesterol were performed on dialyzed and lyophilized SLO samples. No cholesterol could be detected by this method in samples containing up to 200 μg protein. The detection limit in this assay was ca. 2.5 μg of cholesterol per 100-μl sample. Thus, the isolated SLO oligomers could contain no more than 1 to 1.5% cholesterol by weight.

Ultrastructure of membrane-derived SLO. Negative staining of sucrose gradient fractions containing the membrane-derived toxin revealed numerous 7- to 8-nm-broad, curved rods with a 13- to 16-nm inner radius of curvature (Fig. 4). The length of the rods varied from 25 to 100 nm, the latter corresponding to closed ring structures of about 26-nm inner diameter. Most rods were approximately semicircular. A faint stain deposit was discerned in the middle of the rods along their full length. The concave side of the rods always appeared smooth and sharply contoured, whereas small irregular tufts were generally seen on the convex side. Rods

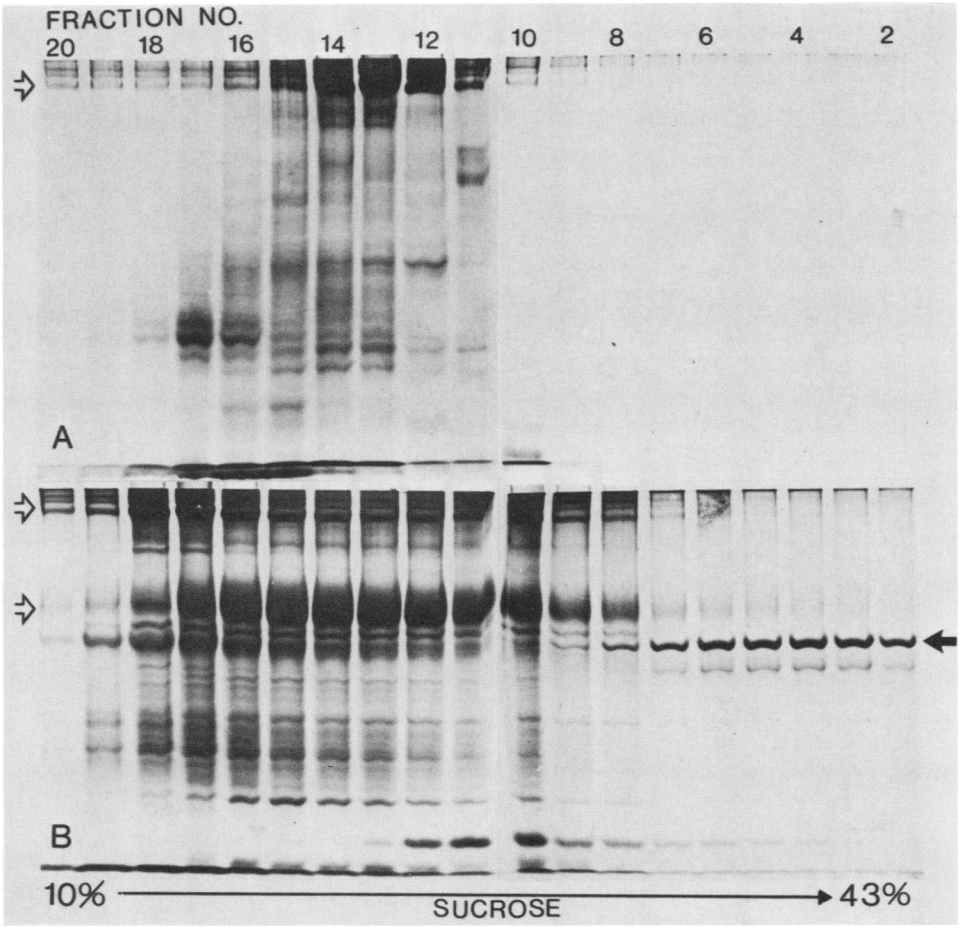

FIG. 3. Non-elutability of SLO from membranes with dilute EDTA at pH 8.0. SLO-treated human erythrocyte membranes were eluted with 1 mM EDTA, pH 8.0. The EDTA eluate (A) and the EDTA pellet (B) were treated with 250 mM DOC and centrifuged through sucrose density gradients (direction of sedimentation, left to right). Twenty fractions were collected, and samples were analyzed by SDS-PAGE. Extraction with EDTA liberated the spectrins (A, open arrow) and other peripheral proteins but none of the SLO oligomers; these were recovered together with the band 3 (and other) integral membrane protein(s) in the EDTA pellet (B; open arrows point to spectrin [top] and band 3 protein [bottom]). Note again the separation of SLO (solid arrow) from other proteins.

devoid of such tufts were, however, also observed (Fig. 4C). The rods showed a distinct tendency to form small aggregates by adherence along their convex sides or at their ends.

The structure of membrane-derived, delipidated SLO thus fully conformed to the spectrum of arc-shaped lesions formed by the toxin on erythrocytes (Fig. 5) (13, 15).

Protease resistance of membrane-derived SLO. Membranes carrying SLO and detergent-solubilized, isolated SLO preparations were extensively proteolysed by trypsin plus chymotrypsin at enzyme/protein ratios of 1:50 (4 h, 20°C). No alteration of ultrastructure or sedimentation properties of the SLO oligomers was observed after such treatment (Fig. 5B), although limited proteolysis was observed by SDS-PAGE (not shown). Oligomerized SLO thus shares with C5b-9(m) and staphylococcal α-toxin hexamers the property of protease resistance (9a). In contrast, native SLO was rapidly degraded by trypsin, and degradation was paralleled by total loss of hemolytic activity (data not shown).

Reincorporation of SLO oligomers into phosphatidylcholine liposomes. When isolated membrane-derived SLO was mixed with DOC-solubilized egg lecithin and the DOC was subsequently removed by dialysis, the protein became firmly associated with the lipid vesicles formed and was recovered in lipid-bound form after flotation of the liposomes in sucrose density gradients. In the electron microscope, the curved rods were found to be incorporated in the liposomal membranes and to exhibit the full spectrum of lesions observed on SLO-treated erythrocytes, including circular, semicircular, twinned, and clustered forms (Fig. 6). Of particular interest was the observation that when rods were not part of closed profiles, what appeared as a free edge of liposomal membrane extended between the ends of a given rod (Fig. 6D through G). Occasionally, such free edges extended as a tongue onto the carbon film substrate of the grid surface from such sites (Fig. 6H). When twinned forms were seen bent over the edge of a liposome, the absence of a membranous diaphragm spanning the lesion was evident (Fig. 6L and M). These observations are in full accordance with the observation of similar, apparently free edges of membrane in SLO lesions on erythrocytes (Fig. 5). When lesions were observed in profile or as oblique projections along the edges of liposomes, the material of the rods appeared slightly elevated relative to the membrane surface (Fig. 6B, C, and D). The observation that some rods were partly (Fig. 6K) or fully (Fig. 6B) detached from the liposomes suggested that the rods are rather rigid structures that can be torn from a membrane by the deformations accompanying the negative-staining procedures.

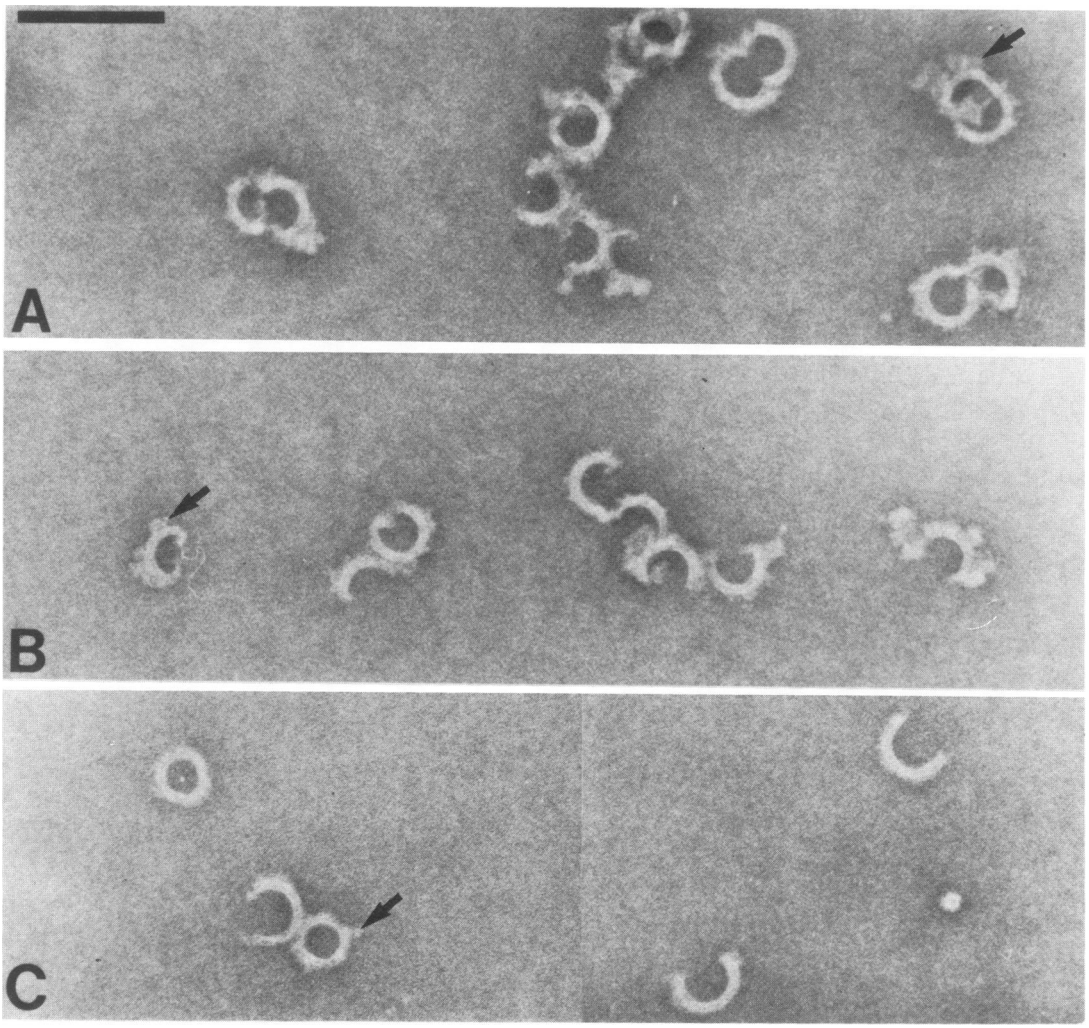

FIG. 4. Electron micrograph of membrane-derived SLO recovered in detergent-solubilized and delipidated form from a sucrose density gradient. A, B, and C correspond to 36S, 30S, and 26S fractions, respectively. The toxin oligomers form 7- to 8-nm-broad, curved rod structures, mostly approximately semicircular, but sometimes generating fully closed rings. The rods tend to adhere at their ends and at their convex sides, which carry some irregular tufts (arrows). (C) has been selected to show rods with few or no such tufts. Sodium silicotungstate staining. Bar, 100 nm.

Freeze-fracture electron microscopy. Rotary-shadowed freeze-fracture replicas of SLO-treated erythrocytes revealed the presence of curved rod structures slightly elevated relative to the lipid plateau of fracture E-faces, dimensionally fully compatible with the SLO-induced lesions observed by negative staining (Fig. 7A). In etched preparations, the small areas of membrane delineated by the elevated rods were generally free of platinum deposits, suggesting a defect in the outer membrane leaflet at these sites. Fracture P-faces (Fig. 7B) revealed dimensionally corresponding, sharply punched defects in the inner membrane leaflet. These defects were deepened by etching up to a depth at which platinum was not deposited at their bottoms. On the true outer cell surface (ES), slightly elevated annular structures were present as disclosed by deep etching (Fig. 7C).

DISCUSSION

SLO is considered the prototype of a large group of bacterial toxins that damage cholesterol-containing target membranes (1, 2, 4, 5, 25). We sought to isolate membrane-bound SLO, define its structure and composition, particularly with respect to cholesterol content, and determine its molecular nature with regard to hydro- or amphiphilicity. The collective data presented in this study indicate that SLO, after binding to a cholesterol-containing membrane, self-associates to form curved, rod-shaped oligomers that are amphiphilic and that penetrate into the apolar domains of the membrane. The convex sides of these rods carry apolar surfaces since they associate with lipid. This association appears to be nonspecific because isolated toxin oligomers bind tightly to phosphatidylcholine in the absence of measurable amounts of cholesterol. The concave sides appear to be hydrophilic. Embedment of ring-shaped SLO oligomers generates protein-lined transmembrane channels of 25- to 30-nm internal diameter. Embedment of noncircularized rods appears to create slits or large apertures in the bilayer, which we believe arise through repelling of membrane fatty acid chains away from the hydrophilic, concave surface of the structures. A hypothetical model for the arrangement of membrane lipid molecules in these areas is shown in Fig. 8. In all cases, therefore, the burial of SLO oligomers within

the bilayer creates large membrane defects, and this, we propose, forms the molecular basis of membrane damage by the toxin. In accordance with earlier studies (15), we observed that two individual, noncircularized rods were sometimes joined at their ends to form very large lesions measuring up to 65 nm in one dimension.

The C-shaped or circular SLO structures have previously been thought to represent SLO-cholesterol complexes (1, 4), and much effort has been devoted to the determination of cholesterol/SLO molar ratios in various experimental systems in the past. However, our results indicate that cholesterol does not contribute significantly to the actual membrane-derived SLO structure. We have no evidence to indicate that SLO rods contain constituents other than the SLO molecules themselves. The nature of the tufts adhering to the convex sides of the rods requires further study; at present, neither SDS-PAGE nor lipid analyses indicate that they represent residual, tightly bound membrane protein or lipid. Our observation that SLO oligomers contain very little (less than 1 to 1.5% by weight) or possibly no cholesterol is consistent with a recent report showing spontaneous formation of similar structures by tetanolysin at high concentration in the absence of any membrane target (22). With Rottem et al. (22) and Cowell et al. (12), we agree that membrane cholesterol probably facilitates the concentration of such toxins on target cell surfaces to a putative threshold that allows oligomerization to take place. It is of interest to note that spontaneous oligomerization of channel-forming proteins to form the typical ring and cylinder structures in solution has been found also for the C9 complement component (29) and for staphylococcal α-toxin (3). This property thus reflects a potential capacity of the molecules to self-assemble under the appropriate experimental conditions.

Volume calculations based on electron microscopy indicate a volume of approximately 6,000 nm^3 for a typical closed SLO ring, corresponding to a molecular weight of about 5×10^6 (assuming a partial specific volume of 0.73). Since the molecular weight of native SLO is 69,000, we estimate that such closed ring structures harbor 70 to 80 molecules of SLO monomers. As discussed in a previous communication, the hemolytic capacity of SLO is consistent with the concept that one or very few oligomer lesions will induce lysis of an erythrocyte (8). It should be mentioned that the present studies were conducted with high toxin doses (50 μg of toxin per 10^9 cells). The structure of the lesions induced by low, just lytic doses has not been studied. For cereolysin, a related sulfhydryl-activated toxin, Cowell et al. (12) obtained indications that the lesions induced at low, hemolytic toxin concentrations may differ structurally from those formed at high concentrations. It is possible that the basic principle of lesion formation is the same but that the oligomers forming under low toxin doses harbor fewer toxin molecules, and some functional lesions may then not be visible in the electron microscope.

Our collective ultrastructural data clearly speak for the formation of large transmembrane pores at the toxin doses applied in this study. The indications for the presence of holes, partly or fully lined by toxin arcs or rings on erythro-

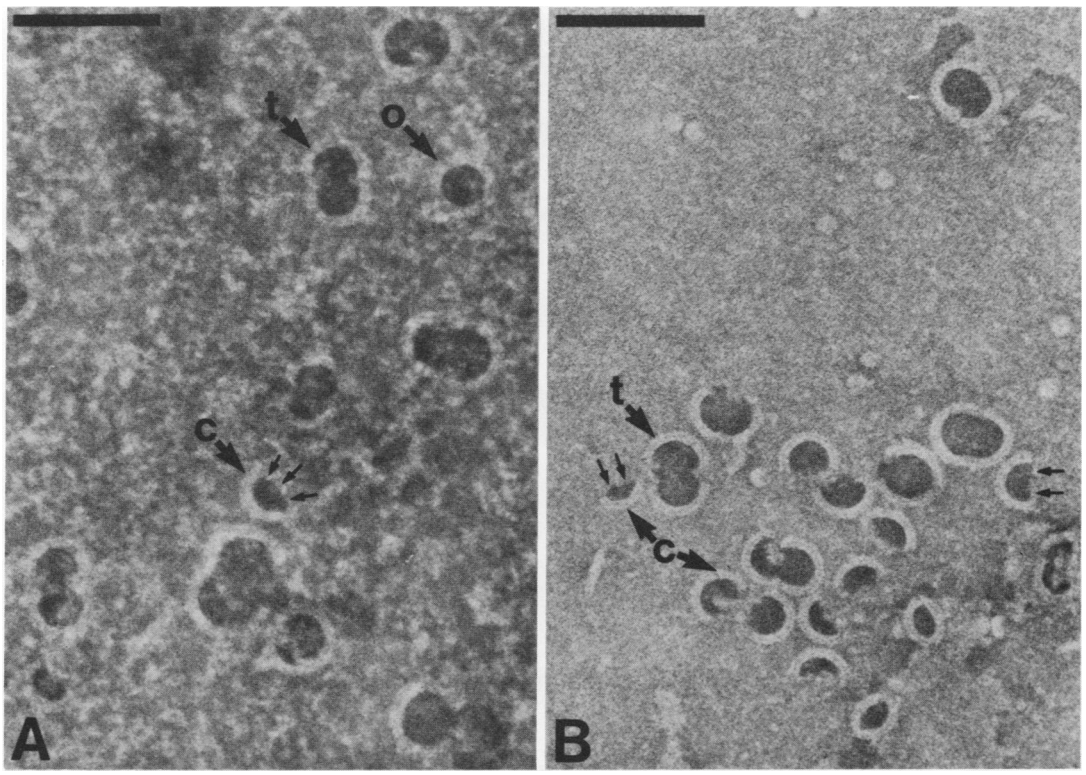

FIG. 5. Electron micrographs of erythrocytes lysed with SLO. (A) Membrane immediately after lysis; (B) membrane from the same preparation after prolonged treatment with trypsin plus chymotrypsin, which removes most extraneous membrane material but does not destroy the SLO oligomers. The SLO lesions are seen as 7- to 8-nm-broad, arc-shaped structures in semicircular (c), circular (o), and twinned (t) configurations. Dense stain deposits are bordered by the sharply contoured concave side of the arcs. When arcs do not form closed profiles, part of the circumference of the stain deposit is bordered by an apparently free edge of membrane extending between the ends of a given arc, as indicated by small arrows. Sodium silicotungstate negative staining. Bars, 100 nm.

cytes, were fully corroborated by the observations made on reconstituted liposomal membranes. Contrary to earlier findings on the cereolysin lesions (12), we also found that SLO induces defects in the lipid plateau of fracture P-faces that could be deepened by etching. Taken together with the finding of ring and arc structures on fracture E-faces and on the outer cell surface which fully corresponded in dimensions to the structures defined by negative staining, the freeze-fracture data supported the contentions reached from the negative-staining analyses. Our data are in complete accord with the functional studies of Duncan et al. (11, 14), who have demonstrated the presence of very large lesions in toxin-treated membranes that permit the escape of macromolecules of ≥15 nm effective molecular diameter from the cells. The functional data of Buckingham and Duncan (11) and the present structural data are also in accord with the finding that SLO-treated erythrocytes do not undergo osmotic lysis (11), as has been found for hemolysis induced by complement (18, 24) and staphylococcal α-toxin (6). In the latter cases, the transmembrane channels are not large enough to permit direct escape of hemoglobin. Influx of water and small ions thus ensues via the Donnan equilibrium, the cells undergo osmotic swelling, and the membranes eventually rupture and release the hemoglobin (9a).

It is most probable that many, if not all, other toxins that belong to the class of sulfhydryl-activated cytolysins function in the same manner as SLO, and their isolation from membrane targets is likely to be possible by using the simple methods described in this paper. Additional studies may provide further insights into the process of transmembrane pore formation. It appears intriguing that insertion of molecules with hydrophobic surfaces aligned on one side and with hydrophilic surfaces on the other may create leaks in the membrane by repelling lipid away from the hydrophilic areas. It appears worthwhile to consider the possibility that such a principle may be operative in some other cases of transmembrane pore formation, as for example with incompletely assembled terminal complement complexes (8a), with certain colicins (20), or even in the case of protein domains mediating translocation of adjacent polypeptides

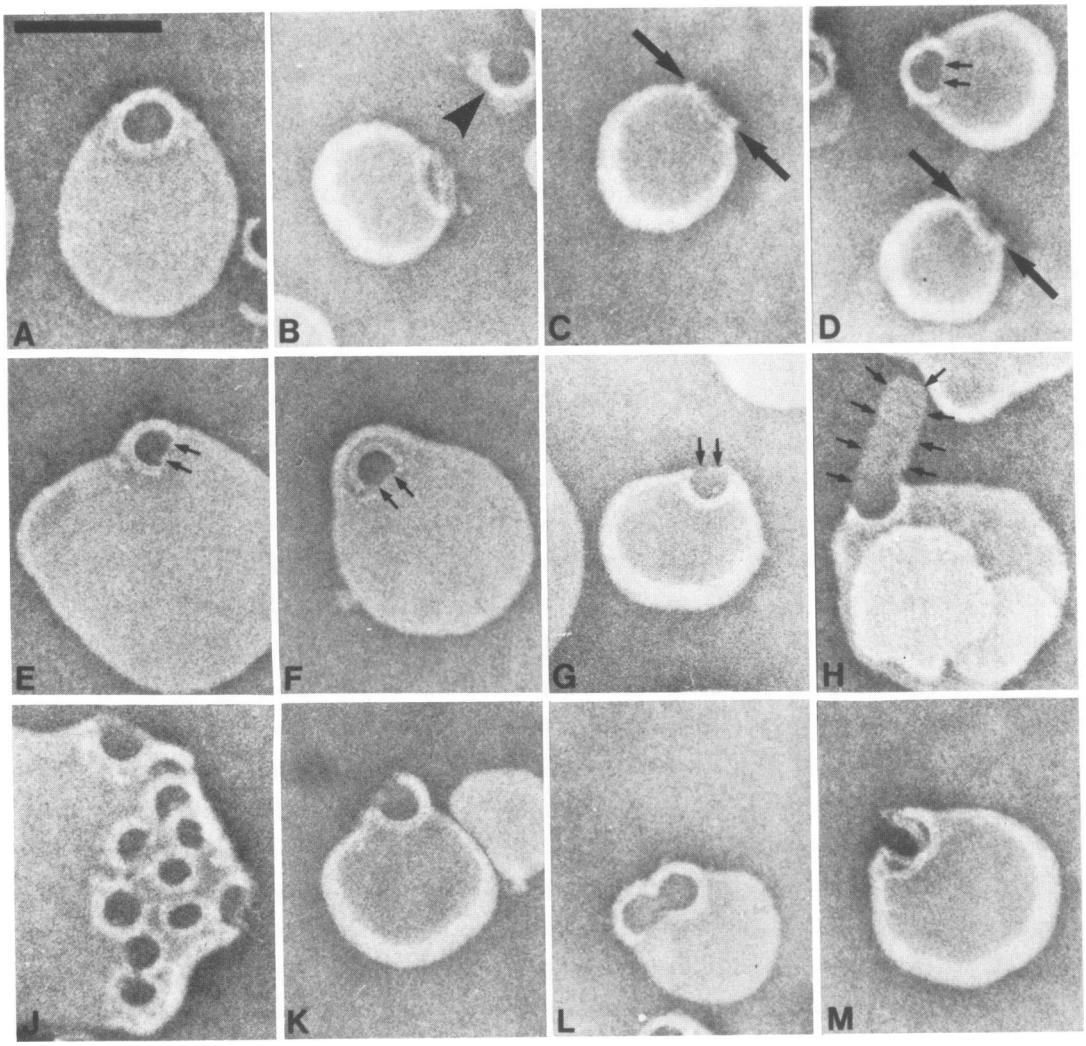

FIG. 6. Negatively stained phosphatidylcholine liposomes carrying reincorporated SLO oligomers. The liposomes carry lesions identical to those induced by native SLO on erythrocyte membranes, including circular (A), semicircular (e.g., F), twinned (L), and clustered (J) forms. In oblique and side projections (B, C, D), the rod structures appear slightly elevated relative to the membrane surface. Small arrows in D through H indicate free edges of liposomal membrane extending between ends of semicircular rods. Arrowhead in B indicates a detached SLO rod. Sodium silicotungstate negative staining. Bar, 100 nm.

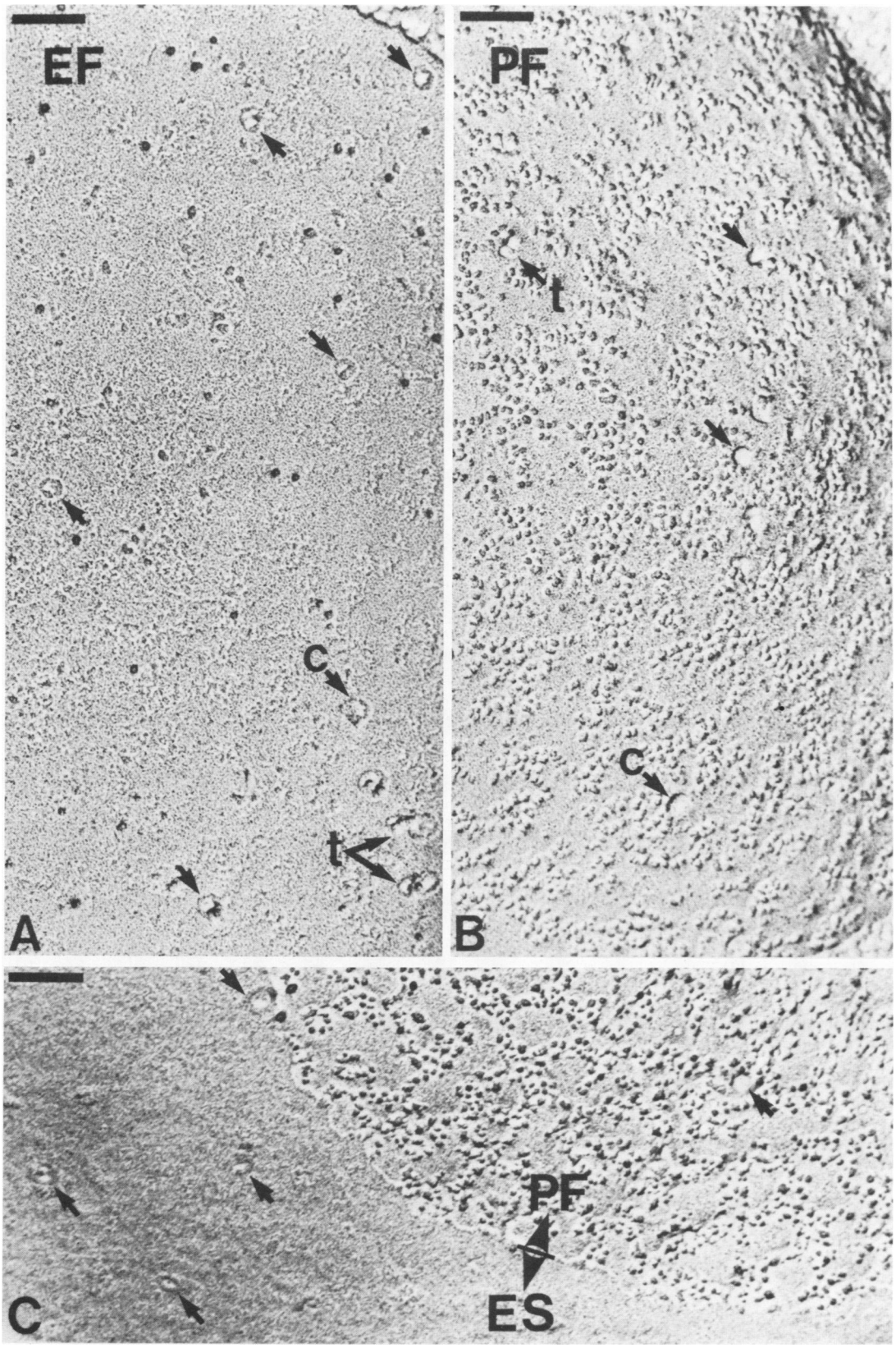

FIG. 7. Rotary-shadowed freeze-fracture replicas of erythrocytes lysed by SLO. A and B derive from membranes, fixed in glutaraldehyde and cryoprotected in glycerol, whereas the membrane in C was unfixed and frozen in 5 mM phosphate buffer. Fracture E-faces (A) exhibit rings and semicircular (c) structures elevated relative to the lipid plateau. Some rings are twinned (t). Fracture P-faces (B and C) exhibit distinct defects in the lipid plateau. Some of these appear sharply and steeply contoured at one side while fading at the opposite side (e.g., lesions labeled c). Some defects occur in pairs (t). ES-faces (C) exhibit circular and semicircular structures slightly elevated relative to the membrane surface. Bars, 100 nm.

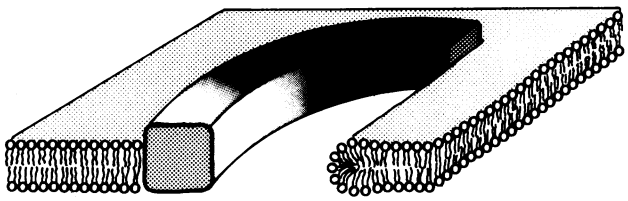

FIG. 8. Diagrammatic presentation of the gross, principle features proposed for the SLO-induced membrane lesion generated by incompletely circularized toxin oligomers.

such as occurring during the transport of enzymatically active toxin fragments (e.g., diphtheria toxin A [21, 23]) across the bilayer.

ACKNOWLEDGMENTS

We thank Marion Muhly and Margit Pohl for excellent technical assistance.

These studies were supported by the Deutsche Forschungsgemeinschaft (Bh 2/2).

LITERATURE CITED

1. **Alouf, J. E.** 1980. Streptococcal toxins. Pharm. Ther. **11**:661–717.
2. **Alouf, J. E., and C. Geoffroy.** 1984. Structure-activity relationships in sulfhydryl-activated toxins, p.165–172. *In* J. E. Alouf, F. J. Fehrenbach J. H. Freer, and J. Jeljaszewicz (ed.), Bacterial protein toxins. Academic Press, London.
3. **Arbuthnott, J. P., J. H. Freer, and A. W. Bernheimer.** 1967. Physical states of staphylococcal α-toxin. J. Bacteriol. **94**:1170–1177.
4. **Bernheimer, A. W.** 1974. Interactions between membranes and cytolytic bacterial toxins. Biochim. Biophys. Acta **344**:27–50.
5. **Bernheimer, A. W.** 1976. Sulfhydryl-activated toxins, p. 85–97. *In* A. W. Bernheimer (ed.), Mechanisms in bacterial toxinology. John Wiley & Sons, Inc., New York.
6. **Bhakdi, S., M. Muhly, and R. Füssle.** 1984. Correlation between toxin binding and hemolytic activity in membrane damage by staphylococcal α-toxin. Infect. Immun. **46**:318–323.
7. **Bhakdi, S., M. Muhly, and M. Roth.** 1983. Isolation of specific antibodies to complement components. Methods Enzymol. **93**:409–420.
8. **Bhakdi, S., M. Roth, A. Sziegoleit, and J. Tranum-Jensen.** 1984. Isolation and identification of two hemolytic forms of streptolysin-O. Infect. Immun. **46**:394–400.

8a. **Bhakdi, S., and J. Tranum-Jensen.** 1984. On the cause and nature of C9-related heterogeneity of C5b-9 complexes generated on target erythrocyte membranes through the action of whole serum. J. Immunol. **133**:1453–1563.

9. **Bhakdi, S., and J. Tranum-Jensen.** 1978. Molecular nature of the complement lesion. Proc. Natl. Acad. Sci. U.S.A. **75**:5655–5659.

9a. **Bhakdi, S., and J. Tranum-Jensen.** 1984. Mechanism of complement cytolysis and the concept of channel-forming proteins. Phil. Trans. R. Soc. London B **306**:311–324.

10. **Bhakdi, S., J. Tranum-Jensen, and Z. Sziegoleit.** 1984. Structure of streptolysin-O in target membranes, p. 173–180. *In* J. E. Alouf, F. J. Fehrenbach, J. H. Freer, and J. Jeljaszewicz (ed.), Bacterial protein toxins. Academic Press, London.
11. **Buckingham, L., and J. L. Duncan.** 1983. Approximate dimensions of membrane lesions produced by streptolysin-S and streptolysin-O. Biochim. Biophys. Acta **729**:115–122.
12. **Cowell, J. L., K. S. Kim, and A. W. Bernheimer.** 1978. Alteration by cereolysin of the structure of cholesterol-containing membranes. Biochim. Biophys. Acta **507**:230–241.
13. **Dourmashkin, R. R., and W. F. Rosse.** 1966. Morphological changes in the membranes of red blood cells undergoing hemolysis. Am. J. Med. **41**:699–710.
14. **Duncan, J. L.** 1974. Characteristics of streptolysin O hemolysis: kinetics of hemoglobin and ^{86}rubidium release. Infect. Immun. **9**:1022–1027.
15. **Duncan, J. L., and R. Schlegel.** 1975. Effect of streptolysin-O on erythrocyte membranes, liposomes, and lipid dispersions. A protein-cholesterol interaction. J. Cell Biol. **67**:160–173.
16. **Fairbanks, G., T. L. Steck, and D. F. H. Wallach.** 1971. Electrophoretic analysis of the major polypeptides of the human erythrocyte membrane. Biochemistry **10**:2606–2617.
17. **Füssle, R., S. Bhakdi, A. Sziegoleit, J. Tranum-Jensen, T. Kranz, and H. J. Wellensiek.** 1981. On the mechanism of membrane damage by *S. aureus* α-toxin. J. Cell Biol. **91**:83–94.
18. **Green, H., P. Barrow, and B. Goldberg.** 1959. Effect of antibody and complement on permeability control in ascites tumor cells and erythrocytes. J. Exp. Med. **110**:699–712.
19. **Harboe, N., and A. Ingild.** 1973. Immunisation, isolation of immunoglobulins. Estimation and antibody titer. Scand. J. Immunol. **2**(Suppl. 1):161–164.
20. **Konisky, J.** 1982. Colicins and other bacterioicins with established modes of action. Annu. Rev. Microbiol. **36**:125–144.
21. **Pappenheimer, A. M., Jr.** 1977. Diphtheria toxin. Annu. Rev. Biochem. **46**:69–94.
22. **Rottem, S., R. M. Cole, W. H. Habig, M. F. Barile, and M. C. Hardegree.** 1982. Structural characteristics of tetanolysin and its binding to lipid vesicles. J. Bacteriol. **152**:888–892.
23. **Sandvig, K., and S. Olsnes.** 1980. Diphtheria toxin entry into cells is facilitated by low pH. J. Cell Biol. **87**:828–832.
24. **Sears, D. A., R. Weed, and S. L. N. Swisher.** 1964. Differences in the mechanism of in vitro immune hemolysis related to antibody specificity. J. Clin. Invest. **43**:975–985.
25. **Smyth, C. J., and J. L. Duncan.** 1978. Thiol-activated (oxygen-labile) cytolysins, p. 129–183. *In* J. Jeljaszewicz and T. Eadström (ed.), Bacterial toxins and cell membranes. Academic Press, Inc., New York.
26. **Smyth, C. J., J. H. Freer, and J. P. Arbuthnott.** 1975. Interaction of *Clostridium perfringens* haemolysin, a contaminant of commercial phospholipase C, with erythrocyte ghost membranes and lipid dispersions. Biochim. Biophys. Acta **382**:479–493.
27. **Steck, T. L.** 1974. The organisation of proteins in the human red blood cell membrane. J. Cell Biol. **62**:1–19.
28. **Tranum-Jensen, J., S. Bhakdi, B. Bhakdi-Lehnen, O. J. Bjerrum, and V. Speth.** 1978. Complement lysis: the ultrastructure and orientation of the C5b-9 complex on target sheep erythrocyte membranes. Scand. J. Immunol. **7**:45–56.
29. **Tschopp, J., H. J. Müller-Eberhard, and E.R. Podack.** 1982. Formation of transmembrane tubules by spontaneous polymerization of the hydrophilic complement protein C9. Nature (London) **298**:534–537.